

Photoluminescence studies of the charge states of nitrogen vacancy centers in diamond after arsenic ion implantation and subsequent annealing

Mrs. B. Santhoshi, Mr. B. Srinidhi, Mr. N. Sudhakara rao, Ms. V. Mounika

Assistant Professor, HOD^{1,2,3}, Assistant Professor⁴

KGRL COLLEGE (A) PG COURSES, BHIMAVARAM.

ABSTRACT

Photoluminescence spectroscopy was used to examine the nitrogen vacancy (NV) centres of high nitrogen diamond implanted with arsenic ions in this study. Consistent changes in laser excitation power and measurement temperature after high-temperature annealing were used to explain the NV centre charge state shift. The NV yield is reduced because the amorphous layer created by arsenic ion implantation becomes a graphitization layer after high-temperature annealing. The centres of electric neutral NV (NV⁰) and negatively charged NV (NV⁻) are impacted by radiation recombination and Auger recombination as the power of the laser increases. The intensities of NV centres declined and finally quenched as the measuring temperature increased. Furthermore, a change was taking place in the charge states of the NV⁻ and NV⁰ centres. As a result of the preponderance of electron-phonon interaction in the displacement of diamond energy gaps as a function of temperature, the red shift in the zero phonon line locations of NV centres was also explained. As the temperature increased, the NV center's entire width at half maximum widened considerably.

I. INTRODUCTION

II. The unique features of diamond's nitrogen vacancy (NV) centres make them a promising material for the development of new quantum devices, including quantum computers and communication qubits.^{1,2} It might be useful in many future quantum state engineering and

magnetic sensor projects.^{3,4} because of phenomena like optical transitions in solid-state electronics and its apparent atomic-like characteristics, as well as its long-lived spin quantum state.⁵ Ion implantation or post-irradiation annealing may produce the NV centres. Creating NV centres adjacent to a surface is most often accomplished by low energy ion implantation (6, 7).^{8, 9} Additionally, ion implanted NV centres with a shallow surface exhibit superior sensitivity and resolution, making them an obvious superior research tool.^{10,11} Creating NV centres near the surface is necessary for coupling to optical structures, according to Santori et al., who studied the impact of gallium ion implantation and annealing on the vertical distribution of NV centres.¹² The optical coherence of NV centres is connected to the formation location and lattice damage, rather than the inherent properties of diamonds, according to Van Dam et al., who formed NV centres via nitrogen ion implantation followed by high-temperature annealing. In order to increase the production of NV, Naydenov developed a technique that employed the ¹⁵N isotope to differentiate between NV centres formed from diamonds' leftover nitrogen (¹⁴N).¹⁴ Pezzagna found that the yield for NV centre production rose with the ion energy throughout the complete investigated range of less than 1% to approximately 50%.¹⁵

As stated in Reference 16, the energy level of the donor for diamonds with substituted As is below the value of the minimum conduction

band of 0.4 eV, much lower than that of reduced P. As a result, mathematically speaking, it is a shallow donor. Prior research confirmed that diamond contains n-type dopant at a shallow depth. The number of Research on the existing form in diamonds and the As dopant also had an important role in the development of n-type diamonds. Sun¹⁸ shown that arsenic impurity is a competitive candidate material for n-type doped diamond by using density functional theory to compute and describe the substitution defect structure of arsenic doped diamond. It is challenging for arsenic atoms to penetrate the lattice as replacements because of their very poor solubility and high ion radius.¹⁹ After high radius ion implantation, it is difficult to both create and observe changes in the charge states of NV centres. Hence, the As dopant was introduced into diamond by ion implantation, and the impact on the charge state of NV centres inside the diamond was studied.

III. EXPERIMENTAL METHODS

IV. A $3 \times 3 \times 0.5$ mm³ diamond, created at Xi'an Jiaotong University, China, using high-temperature high-pressure (HTHP) synthesis, is the main subject of this study. There are more than 20 parts per million of nitrogen impurities. Afterwards, 5×10^4 cm⁻² of arsenic ions were injected onto the (100) surface on the sample's right-angle side using the French IBS ICM-200 ion implantation machine. The injection was done at room temperature, with an incidence angle of 7°, using an energy of 130 keV. A black layer formed in the diamond's As ion implantation region because the implanted arsenic ions were deposited on the surface, which is caused by the enormous covalent radius of the ions. After that, the diamond with ions implanted was heated to 1350 °C for 60 minutes in an argon-circulating annealing chamber. After annealing, the severely amorphous layer became a graphitization layer, and this change was proportional to the recoverable vacancy concentration

threshold.^{20,21}

The next step was to analyse the substance using a Linkam THMS600 low-temperature cooling stage attached to a Renishaw confocal Raman microscope. To get the reading from 80 K to room temperature, one has to precisely change the measuring temperature and regulate the flow rate of liquid nitrogen. An Nd-YAG semiconductor laser may be excited at a 532 nm wavelength and the chosen laser power can be varied from 50, 25, 5, 2.5, 0.5, 0.25, 0.05, and 0.025 mW, in that order. Using PL spectroscopy to identify the sample's ion implantation surface.

V. RESULTS AND DISCUSSION

VI. Excitation with a 532 nm laser at 80 K and 0.5 mW (1% power level) was used to acquire the PL spectra of high nitrogen diamond before arsenic ion implantation, as shown in Fig. 1. Prior to ion implantation, the NV centres in the spectrum were much more intense than the diamond's typical Raman peak due to large quantities of nitrogen impurities. At 563.2 nm, a zero phonon line (ZPL) with an intensity almost double that of NV0 centres emerged alongside the very high NV centres. Kiflawi²² suggests that the fast crystal growth may have created nitrogen interstitials, which are most likely responsible for the line at 563.2 nm.²³ Figure 2 shows that after ion implantation, the PL optical signal is very weak, with a significant decrease in strength at 563.2 nm and the NV centres, because the As implanted layer overlaps with the damaged black layer close to the surface. The charge states of NV centres were also found to have altered very little after ion implantation compared to prior. The spectral invisibility of diamond's signature peaks suggests that arsenic ions have been effectively implanted into the crystal's surface. Through the use of simulations with the Stopping and Range of implantation depth expectations, the predicted longitudinal range of depths was computed.

VII.

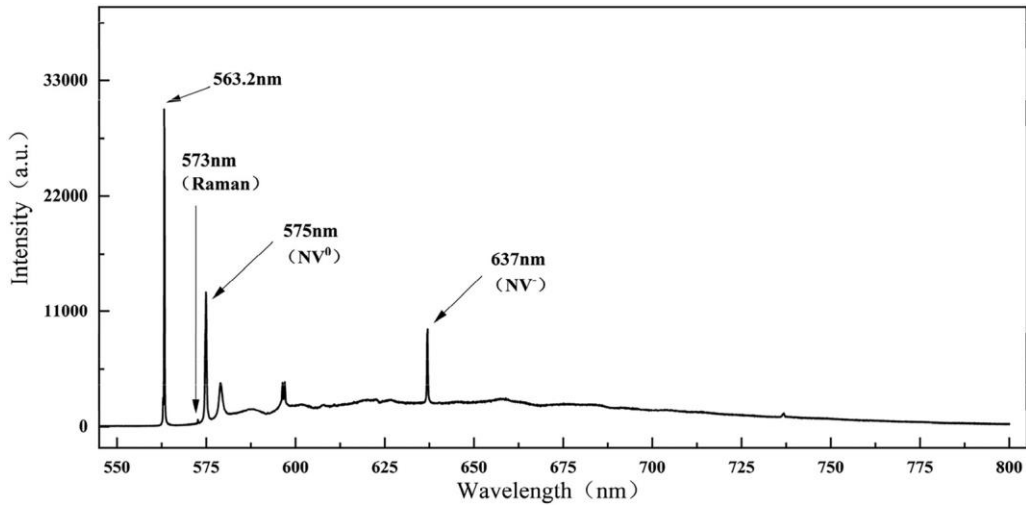


FIG. 1. PL spectra of high nitrogen diamond before arsenic ion implantation recorded at 80 K with a laser excitation wavelength of 532 nm.

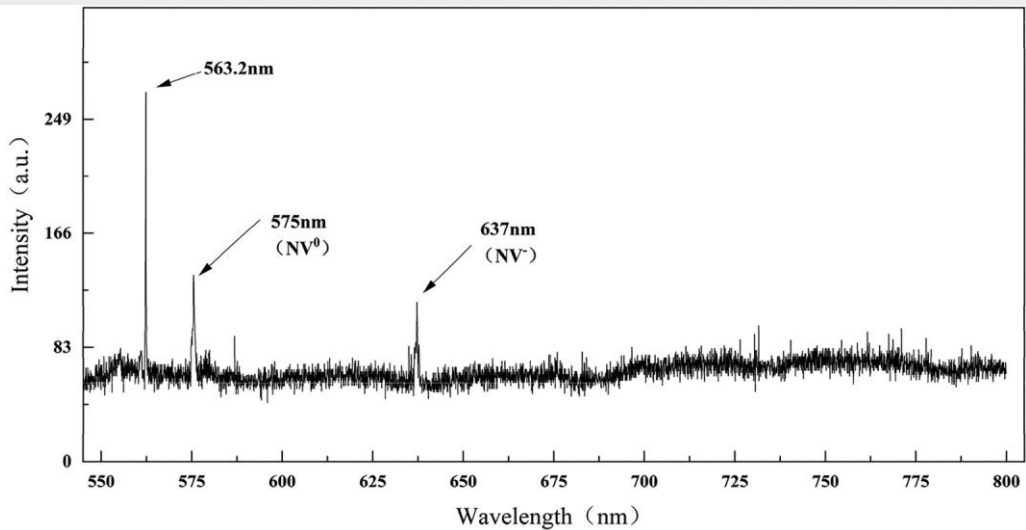


FIG. 2. PL spectra of high nitrogen diamond after arsenic ion implantation recorded at 80 K with a laser excitation wavelength of 532 nm.

Ions in Matter (SRIM) program. For each ion, we forecast damage profiles after implantation at a beam energy of 130 keV using detailed calculations with full damage cascades. Among them, the diamond substrate has a density of 3.515 g/cm^3 . The lattice binding energy is 7.5 eV, surface binding energy is 3.69 eV, and the average displacement energy is 37.5 eV.²⁴ The outputs of ion distribution and damage event calculation at an ion implantation dose of $5 \times 10^{15} \text{ ion cm}^{-3}$ are shown in Fig. 3, simulated the angle of As ion implantation into diamond in this experiment (7°), and the

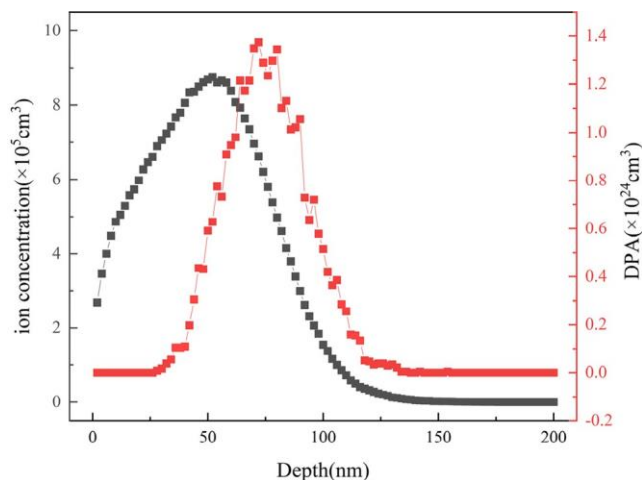


FIG. 3. The effect of SRIM software on predicted ion concentration and dpa with depth at an injection angle of 7°.

displacements per atom (dpa) are computed using the vacancy output of the damage event computations.

As shown in Fig. 3, the projection range of arsenic ions in diamond is quite small. Similar to Pinault’s research,²⁵ when the incident angle is 7°, and the implantation range of arsenic ions is restricted to 30–130 nm (black curve). This means that arsenic ions cannot enter the lattice substitution position or pass through the lattice gap, which means that the injected arsenic ions will only collect on the surface to form the corresponding implantation layer. The associated vacancy density is displayed as a function of injection depth as shown as the red curve; when the injection angle is 7°, the calculated vacancy density exceeds the damage critical threshold by a significant amount ($1 \times 10^{22} \text{ cm}^{-3}$).²¹ The sample exhibits severe graphitization after high-temperature annealing.

After high-temperature annealing, the PL spectra of diamond with arsenic ion implantation are shown in Fig. 4 at

liquid nitrogen temperature. The line at 563.2 nm disappears with the diffusion of nitrogen interstitials after high-temperature annealing.²³ Due to the limitation of measurement intensity, four power levels are measured in the 0.025–0.5 mW range under 532 nm laser excitation. The results indicate that the annealed NV centers exhibit a significant laser power dependence, as shown in Fig. 4(a). The PL intensity of the NV centers is directly proportional to the laser power, and its relationship can be expressed by²⁶

$$I_{PL} \propto P^{\frac{1}{4}} \quad (1)$$

where P is the laser excitation power, and a and k are constants; the PL intensity of the NV centers rises to varied degrees under various excitation circumstances. According to previous research and conclusions, the following equation expresses the directly proportional between the excitation power P and the total of radiation recombination rate (R_L), Auger recombination rate (R_{Aug}), and trap

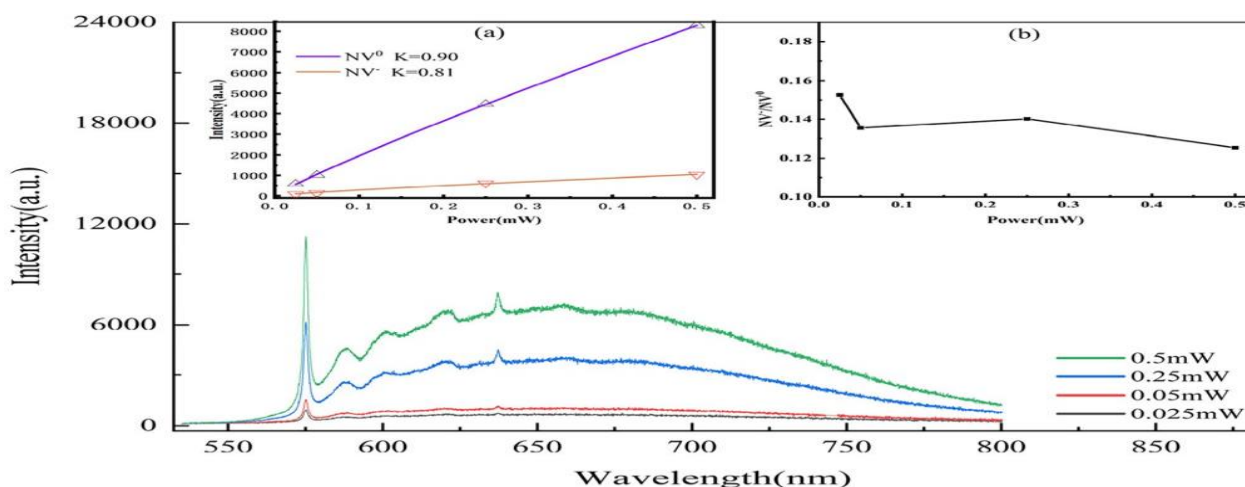


FIG. 4. PL spectra of diamond after arsenic implantation and high-temperature annealing at 80 K using a 532 nm laser at various excitation intensities. (a) PL intensities of NV centers under various excitation powers; (b) the ratio of NV⁻/NV⁰ at various excitation powers.

mediated Shockley read hall recombination rate (R_{SRH}):^{26,27}

$$P \propto R_L + R_{Aug} + R_{SRH}. \quad (2)$$

In actuality, the intensity of PL is influenced by radiation recombination and can be understood as a proportional relationship. Therefore, Eq. (1) can be changed to the following equation:

$$R_L \propto I_{PL} = aP^k. \quad (3)$$

Past research indicates that,³¹ At a k value of 1, the radiation recombination rate (R_L) takes centre stage in Eq. (2), closely aligning with the NV⁰ centre fits to our experimental data. When k=2/3, the Auger recombination rate (R_{Aug}) significantly affects the PL intensity. Equation (2) will be used to obtain the recombination rate (R_{SRH}) when k is equal to 2. Following the non-linear data fitting, the k values of NV⁰ centre were kept at 0.90 and NV⁻ centre at 0.81, respectively. Hence, upon high-temperature annealing of diamonds implanted with arsenic ions, the power dependence of the NV centre laser is primarily affected by the combined effects of radiation recombination and Auger recombination. Auger recombination has a greater impact on the NV⁻ centre compared to the NV⁰ centre.³¹ A graphite layer prevents radiation recombination following laser stimulation, allowing for a greater release of energy via nonradiative recombination. Because of this, we believe that a major component

to a low k value indicates a highly graphitized surface of the crystal. At low temperatures and with 532 nm laser excitation, Fig. 4(b) shows how the central charge state of NV changes as a function of excitation power. Typically, when the excitation power increases, the concentration ratio of the NV⁻

centre to the NV⁰ centre falls, as seen in the figure. The NV⁻ center's electrons are excited by the laser and flow into the conduction band area, where they recombine with vacancies in the valence band. The conversion of NV⁻ centres to NV⁰ centres occurs because the k value tends towards Auger recombination when bound electrons are present.³¹ At the same time, the concentration of NV⁰ centres grows progressively as the laser excitation power increases. The findings of Siyushev et al. are in line with this.²⁸ In Figure 5, the PL spectra of diamond that has been heated to 1350 °C with an excitation power of 0.5 mW are shown, spanning from 80 K to ambient temperature (280 K) using a 532 nm laser. Figure 5 shows that when the measurement temperature rises, the NV centres get stronger. A quenching of NV centres occurs when the excitability of flaws causes them to shift in a specific region. Fig. 5(a) shows the PL intensity data of the NV centres at different measurement temperatures. This shows how the PL intensity of the NV centres relates to the test temperature:²⁹ $I_{PL} = A_0 + B_0 \exp(-E_a/kbT)$, (4)

The thermal quenching activation energies of the diamond NV⁰ and NV⁻ centres are 63 and 96 meV, respectively, whereas E_a is the constant that is used during the transition of the diamond NV centre, kb is the Boltzmann constant, and the constants A₀ and B₀ are also used. The intensity quenching phenomenon occurs as the measurement temperature increases, and the ZPL intensity at the NV centres progressively decreases due to the dominance of nonradiative transitions in the electron emission transition process. The

distance from the excited state minimum to the point where the ground and excited states overlap

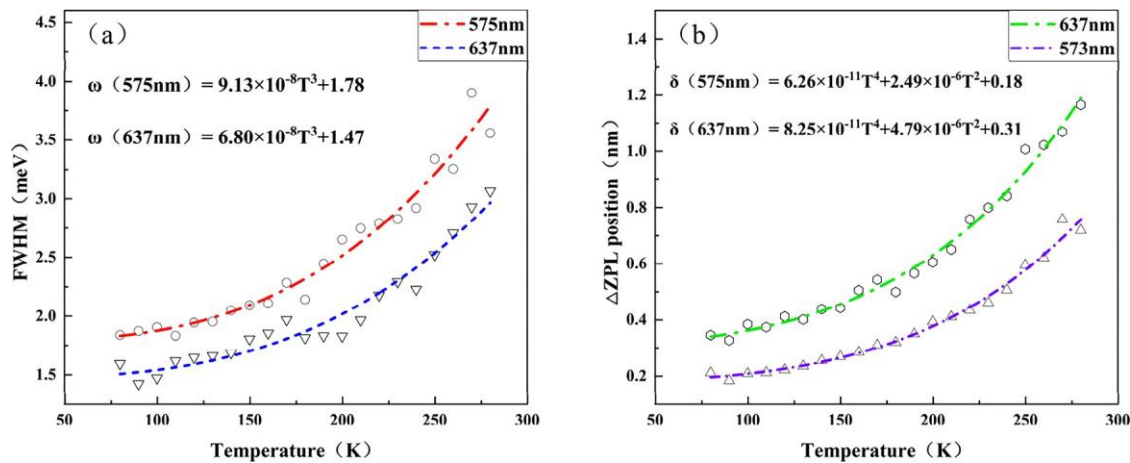


FIG. 6. Temperature-dependent PL spectra of high nitrogen diamond following annealing at 1350 °C. (a) The variation in the ZPL position with temperature; (b) the variation in the FWHM with temperature.

the NV center's activation energy for thermal quenching is given by this number.³⁰ Figure 5(b) shows the intensity ratio of NV charge states (NV⁻/NV⁰) at different measurement temperatures. The fact is shown in Fig. 5(b) that there is a slight but noticeable rising trend in the intensity ratio with increasing observed temperature. The findings of Guo et al. are vastly at odds with this occurrence. As the measuring temperature rose, their report indicated that the NV⁻/NV⁰ ratio remained relatively unchanged.³¹ The fundamental explanation for this difference is because the diamond sample used in Guo's experiment had a very low nitrogen concentration, which meant that the alternative nitrogen atom content was also very low. The diamond sample used for this experiment contains a significant amount of nitrogen. Therefore, when the measurement temperature increases, the charge state between NV centres is affected by a large number of substituted nitrogen atoms. Even though it's possible for some nitrogen atoms to absorb the nitrogen vacancy centre and form nitrogen vacancy defects (NV defects), electrons eventually defrost and migrate, still combining with nearby nitrogen vacancy defects to form nitrogen vacancy centres (NV⁻centres). In the meantime, Groot-Berning detailed phosphorus's and boron's respective behaviours as donors and acceptors.³² Just like phosphorus ion implantation, arsenate ion implantation boosts the stability and yield of NV-centres. Furthermore, because to the amorphization that arsenic ion implantation causes, the sample is unable to recover all of its vacancies after annealing. As a result, the total intensity of the NV charge states is low, ranging from 0.1 to 0.2. Figure 6 displays the trend of the changing temperature on the FWHM and ZPL centres. As the measurement temperature rises, the FWHM also increases, and the ZPL centres exhibit a noticeable red shift phenomena. The FWHM for the NV⁰ and NV⁻ centres, as a function of temperature, is shown in Figure 6(a). Here is the formula that helps explain the variations in these values: $\omega = m_0 + n_0 T^3$, where m_0 and n_0 are constants. The peak redshift of the ZPL centres of NV⁻ and NV⁰ is shown in Fig. 6(b) as the temperature increases, with the highest displacement of the NV⁻ centres being 1.16 nm and the maximum displacement of the NV⁰ centres being 0.75 nm. The combined effects of secondary electron-phonon coupling and lattice expansion cause a linear shift (δE) in the PL spectrum.³³ Where a_0 , b_0 , and c_0 are constants, the linear displacement trend with respect to temperature T may be expressed as $\delta E = a_0 T^4 + b_0 T^2 + c_0$, where $\delta E = \delta E(80\text{ K}) - \delta E(T)$. Lattice vibration and electron-phonon coupling together account for T^4 , whereas the thermal softening effect of the chemical bond is responsible for T^2 . A reduced ZPL displacement was thought by Guo et al. to be responsible for the increased "hardness"³¹ of diamond

atomic structures with fault features. Thus, we likewise hold the belief that the NV0 centres in this experiment exhibit a greater "hardness" compared to the NV⁻ centres.

VIII. CONCLUSION

IX. To review, high-temperature annealing of high-nitrogen diamond implanted with arsenic ions was followed by photoluminescence investigations on the temperature dependency of the pertinent NV centres. Arsenic ion implanted diamonds show a significant degree of graphitization during high-temperature annealing. The findings show that bound electrons and diamond graphitization drive the sublinear development in NV centres as the power of the laser rises, whereas radiation recombination and Auger recombination work together on the NV0 and NV⁻ centres. The level of ionisation conversion of the NV⁻ centres, however, is not very great when contrasted with low nitrogen diamond. Furthermore, the concentration of NV⁻ centres is greater than that of NV0 centres as the measurement temperature rises. This is because NV⁻ centres are formed when electrons from surrounding NV defects are used by high nitrogen diamonds, which are known for their high concentration of N0. The change in the NV⁻/NV0 ratio, however, is not huge, and the temperature is strongly related to the displacement of ZPLs and the rise in the FWHM. For the best match with the curve of $\ddot{v} = m0 + n0T^3$, the expanding FWHM of ZPL is the most appropriate. As the temperature rises, the red shift of ZPLs caused by lattice expansion and stronger electron-phonon coupling may be expressed as $\delta E = a0T^4 + b0T^2 + c0$.

REFERENCES

- Science 276, 2012 (1997) by A. Gruber, A. Dräbenstedt, C. Tietz, L. Fleury, J. Wrachtrup, and C. von Borzyskowski. Proceedings of the Royal Society A 348, 285 (1976), G. Davies and M. F. Hamer. 3 "Appl. Phys. Lett. 75, 3096" (1999) by J. Martin, R. Wannemacher, J. Teichert, L. Bischoff, and B. Köhler. Physics Review B 53, 11360 (1996), 4Y. Mita. Davies et al., Phys. Rev. B 46, 13157 (1992), with additional authors A. T. Collins, S. J. Sharp, S. Mainwood, and G. Davies. Diam. Relat. Mater 16, 1887 (2007) by F. C. Waldermann, P. Olivero, J. Nunn, K. Surmacz, Z. Wang, D. Jaksch, R. Taylor, I. Walmsley, M. Draganski, P. Reichart, A. Greentree, D. Jamieson, and S. Prawer. 7Y. Yu, J. Hsu, K. Chen, and T. Wee, published in J. Phys. Chem. A 111, 9379 in 2007. Article cited as Carbon 30, 294 (2021) by A. Watanabe, T. Nishikawa, H. Kato, M. Fujie, M. Fujiwara, T. Makino, S. Yamasaki, E. D. Herbschleb, and N. Mizuochi. 9H. Ishiwata, M. Nakajima, K. Tahara, H. Ozawa, T. Iwasaki, and M. Hatano, published in the journal Physical Letters, volume 24, issue 043103, in 2017. In a 2015 publication in Nano Letters, S. A. Momenzadeh, R. J. Stöhr, F. F. De Oliveira, A. Brunner, A. Denisenko, S. Yang, F. Reinhard, and J. Wrachtrup were detailed. Eleventh paper published in 2017 by Bourgeois et al. in Physical Review B, with additional authors E. Londero, K. Buczak, J. Hruby, M. Gulka, Y. Balasubramanian, G. Wachter, J. Stursa, K. Dobes, F. Aumayr, M. Trupke, A. Gali, and M. Nesladek. Science of the Physical Review B 79, 125313 (2009) by 12C. Santori, P. E. Barclay, K.-M. C. Fu, and R. G. Beausoleil. 13 In the 2019 issue of Physical Review B, S. B. van Dam, M. Walsh, M. J. Degen, E. Bersin, S. L. Mouradian, A. Galiullin, M. Ruf, M. Ijspeert, T. H. Taminiau, R. Hanson, and D. R. Englund published an article with the DOI: 10.11623. In a 2010 article published in the Physical Review Letters, 14B. Naydenov et al., V. Richter, J. Beck, M. Steiner, P. Neumann, G. Balasubramanian, J. Achard, F. Jelezko, J. Wrachtrup, and R. Kalish were quoted. 15S. Pezzagna, B. Naydenov, F. Jelezko, J. Wrachtrup, and J. Meijer, Article number: 065017 in the New Journal of Physics (2010). The authors of the cited article are J. P. Goss, R. Jones, P. R. Briddon, and S. J. Sque; the publication date is 2004. 17 This is the work of P. W. May, M. Davey, K. N. Rosser, and P. J. Heard, as published in the Materials Research Society Symposium Proceedings, 2008, Volume 1039, page 1501. Diam. Relat. Mater. 108, 107924 (2020) by 18X. Sun, Y. Guo, G. Wu, Y. Zhao, S. Liu, and H. Li. 19 Publication: MRS Proceedings 15, 1039 (2008) by P. W. May, M. Davey, K. N. Rosser, and P. J. Heard.

20Published in 2011 by Physical Review B, this article was written by A. Silverman, J. Adler, and R. Kalish.
21The authors of the article are C. Uzan-Saguy, C. Cytermann, R. Brenner, V. Richter, M. Shaanan, and R. Kalish, and the publication date is 1995. 22Published in Diam. Relat. Mater. 11, 204-211 (2002) by I. Kiflawi, H. Kanda, and S. C. Lawson. In Spectroscopy Letters 53, 270-276 (2020), 23K. Wang, R. Guo, Y. Zhang, and Y. Tian were published. 24“Carbon 157, 97-105” (2020) by E. A. Scott, K. Hattar, J. L. Braun, C. M. Rost, J. T. Gaskins, T. Bai, Y. Wang, C. Ganski, M. Goorsky, and P. E. Hopkins. J. Barjon, 25M.-A. Pinault-Thaury, T. Tillocher, N. Habka, D. Kobor, F. Jomard, J. Chevallier, and J. Barjon. Research in Materials Science and Engineering B 176, 1401-1408 (2011).
26J. Appl. Phys. 123, 015304 (2018) by A. A. ShklyaeV, V. A. Volodin, M. Stoffel, H. Rinnert, and M. Vergnat.
27This is from an article published in 2013 by I. P. Seetoh, C. B. Soh, E. A. Fitzgerald, and S. J. Chua in the Physical Review Letters. 28The article was published in 2013 in the Physical Review Letters by P. Siyushev, H. Pinto, M. Vörös, A. Gali, F. Jelezko, and J. Wrachtrup (2011).
29(J. Appl. Phys. 103, 114908) by M. Benabdesselam, A. Petitfils, F. Wrobel, J. E. Butler, and F. Mady (2008).
Publication: J. Phys. D: Appl. Phys. 53, 135303 (2020), by Wang, R. Guo, S. Ding, H. Wang, Y. Tian, and Y. Wang (30K). 31In the 2020 issue of the Physical Review Letters, R. Guo, K. Wang, Y. Zhang, Z. Xiao, G. Jia, H. Wang, Y. Wu, and Y. Tian were authors. Publication: Phys. Status Solidi A 211, 2268-2273 (2014) by 32K. Groot-Berning, N. Raatz, I. Dobrinets, M. Lesik, P. Spinicelli, A. Tallaire, J. Achard, V. Jacques, J.-F. Roch, A. M. Zaitsev, J. Meijer, and S. Pezzagna. 33Journal of Physics, Volume 34, Pages 149-154 (1967) by Y. P. Varshni. 34Scientific Reports B 234, 644 (2002) by V. Hizhnyakov, H. Kaasik, and I. Sildos. New Journal of Physics 15, 043005 (2013) by 35E. Neu, C. Hepp, M. Hauschild, S. Gsell, M. Fischer, H. Sternschulte, D. Steinmüller-Nethl, M. Schreck, and C. Becher.